

Studies on the Mechanics of Carrier Bead Chains in Two-Component Development Process

Nobuyuki Nakayama

** Key Technologies Development, Technology & Development, Fuji Xerox Co., Ltd.
Nakai-machi, Kanagawa, Japan*

*Satoshi Yamada,** Hiroyuki Takahashi,** Masaya Nakatsuhara,**
Jun Tomomatsu,** Mariko Doi,** and Hiroyuki Kawamoto**
**Department of Mechanical Engineering, Waseda University
Shinjuku, Tokyo, Japan*

Abstract

Three kinds of studies have been carried out on the statics and dynamics of carrier bead chains in an electromagnetic field to solve the three questions, that is, how the mechanical properties of chains are in a high magnetic field, what the effect of friction between beads is, and how the properties of chains vary by the introduction of toner particles. The followings were deduced from the experimental, theoretical and numerical investigations. (1) By the measurement on length and population of chains in the high magnetic field up to 1.0 T, reductions in these properties with the increase in magnetic field were observed in the field more than 0.1 T and the characteristics were confirmed by the numerical calculation with the Distinct Element Method. (2) The observation of chain forming process in oil, where the effect of friction between particles was supposed to be negligible, showed a good agreement with the theoretically estimated value by the assumption of the potential energy minimization. (3) The magnetic effect of toner particles on the chain length is negligible while the electric effect on the electric pull-off properties of chains is significant.

Introduction

A schematic drawing of a two-component development process¹ used for high-speed and/or color laser printers is shown in Fig. 1. Magnetized carrier beads in the magnetic field created by a stationary permanent magnet form chain clusters on a rotatory sleeve. Toner particles attached electrostatically to these magnetic bead chains are transported with rotation of the sleeve. In the development area, electrostatic force acts on toner particles and they move to photoreceptor surface to form real images. The qualities of images closely depend on the properties of chains.

Length, stiffness, and electrostatic pull-off characteristics of the chain have been already investigated in the previous studies²⁻⁴ by experiments with a solenoid coil, theoretical discussion with the assumption of the potential energy minimization,⁵ and numerical simulation of chain forming process by the Distinct Element Method.⁶ It has been clarified how the chain configuration is determined in the magnetic field. However, we still have three questions to be clarified, that is, how the mechanical properties of chains are in an extremely high magnetic field, what the effect of friction between beads is, and how the properties of chains vary by the introduction of toner particles. Then we performed three kinds of experimental, theoretical and numerical studies. One was the observation and calculation of chain formation under high magnetic field created by a superconducting coil that created field up to 1.0 T. The second was a chain formation experiment in oil to reduce an effect of friction between the beads and the last was measurement of the length and electrostatic pull-off characteristics of carrier bead chains with toner particles.

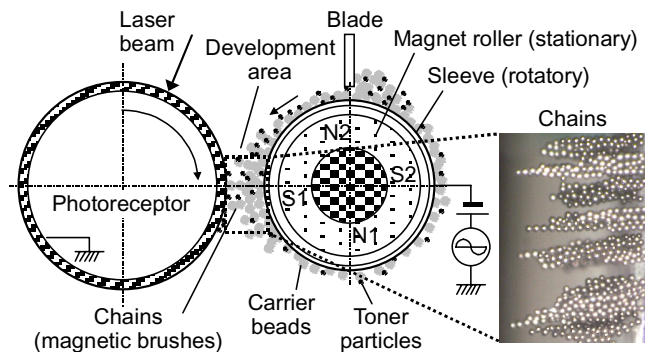


Figure 1. Two-component development process for laser printers.

Motion of Carrier Beads in a Magnetic Field

Basic Equation

The 3D momentum equation of a bead j in a magnetic field with six degrees of freedom, $(x, y, z, \theta_x, \theta_y, \theta_z)$ is expressed by Eq. 1, where (x, y, z) is the Cartesian coordinate vector and $(\theta_x, \theta_y, \theta_z)$ is the rotational angle vector.

$$\begin{aligned} m_j \ddot{\mathbf{x}}_j &= \mathbf{F}_{c_j} + \mathbf{F}_{m_j} + 3\pi\eta a_j \dot{\mathbf{x}}_j + m_j \mathbf{g}, \quad \mathbf{x}_j = (x_j, y_j, z_j) \\ I_j \ddot{\boldsymbol{\theta}}_j &= \mathbf{M}_{c_j} + \mathbf{M}_{m_j}, \quad \boldsymbol{\theta}_j = (\theta_{xj}, \theta_{yj}, \theta_{zj}) \end{aligned} \quad (1)$$

In Eq. 1, mechanical contact force and moment, \mathbf{F}_c and \mathbf{M}_c , the magnetic force and moment, \mathbf{F}_m and \mathbf{M}_m , air drag, and the gravity are considered, where m_j , I_j and a_j are the mass, inertia and diameter of the j -th bead respectively, η is viscous coefficient and \mathbf{g} is gravity acceleration. The equation can be solved numerically by the Distinct Element Method⁶ and motions of beads can be clarified quantitatively.

To discuss the motion of magnetic carrier beads in the magnetic field, magnetic interactions between beads and field is important. Paranjpe discussed these interactions and potential energy.⁵ The magnetic force \mathbf{F}_{mj} to the j -th bead with the magnetic dipole moment \mathbf{p}_j are given by the following expression under the assumption that each bead behaves as a magnetic dipole placed at the center of the bead.

$$\mathbf{F}_{mj} = (\mathbf{p}_j \cdot \nabla) \mathbf{B}_j. \quad (2)$$

The magnetic flux density \mathbf{B}_j at the position of the j -th bead and magnetic moment \mathbf{p}_j are

$$\mathbf{B}_j = \mathbf{B}_j' + \sum_{k=1, k \neq j}^N \frac{\mu_0}{4\pi} \left(\frac{3(\mathbf{p}_k \cdot \mathbf{r}_{kj})}{|\mathbf{r}_{kj}|^5} \mathbf{r}_{kj} - \frac{\mathbf{p}_k}{|\mathbf{r}_{kj}|^3} \right), \quad (3)$$

$$\mathbf{p}_j = \frac{4\pi}{\mu_0} \frac{\mu - 1}{\mu + 2} \frac{a_j^3}{8} \mathbf{B}_j, \quad (4)$$

where N is the number of particles, μ_0 is the permeability of free space, μ is the relative permeability of beads and \mathbf{r}_{kj} is the position vector from the k -th to the j -th bead.

Potential Energy

Stable configurations of chains are supposed to be determined to minimize their potential energy. The total potential energy is given by the sum of magnetic energy U_m expressed by Eq. 5 and gravitational energy.

$$U_m = -\frac{1}{2} \sum_{j=1}^N \mathbf{p}_j \cdot \mathbf{B}_j'. \quad (5)$$

Models for the estimation of potential energy are shown in Fig. 2 that assumes a single chain.

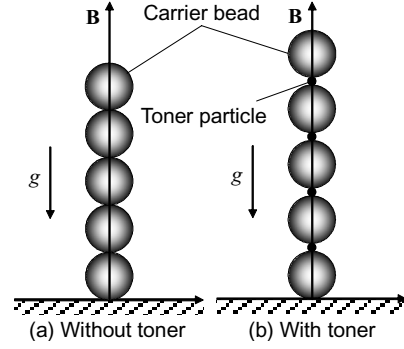


Figure 2. Single chain model for energy estimation.

Chains in a High Magnetic Field

Experimental Method

The observation of chain forming process in a high magnetic field was carried out with a superconducting coil (HF12-100VNT, Sumitomo Heavy Industries, Ltd.) shown in Fig. 3. The coil creates maximum field at 12 T at the center of coil and 1.5 T field at the top of the coil. In the chain formation experiment, the magnetic flux density was swept up and down at 1.87 mT/s rate. Axial component of the field at the top of the coil $B_z(z)$ can be approximated by a linear equation,

$$B_z(z) = B_0(1 - cz), \quad (6)$$

where B_0 ($= 1.47$ T, maximum value at $z = 0$) and c ($= 0.00973$ 1/m) are constants and z (m) is the axial coordinate ($z = 0$ at the top of the coil).

Soft magnetic particles, with 88 μm in diameter, 3620 kg/m^3 in volume density, 4.7 in relative permeability and 0.13-0.64 kg/m^2 in surface loading, were provided in a vessel mounted on the coil. The chain forming process was observed by a digital video camera. The lengths and intervals of the chains were quantified in the recorded images.

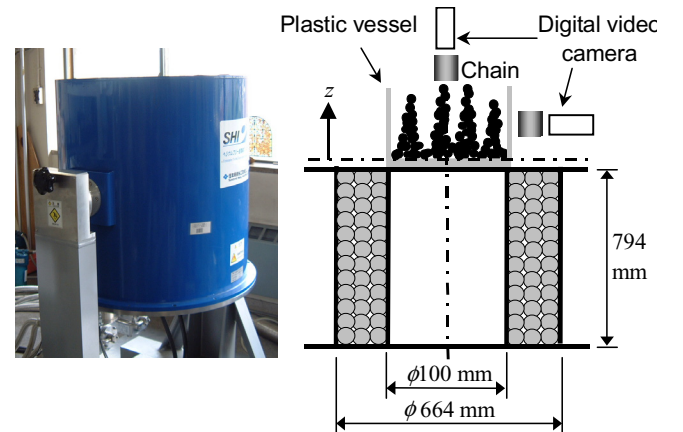


Figure 3. Superconducting coil and experimental setup.

Results

The observed chain profiles are shown in Fig. 4. The length and interval increased with the increase in the magnetic field if the magnetic field is less than 0.1 T, as shown in Fig. 4 (a)-(c). These results were already confirmed in the previous study.² On the other hand, they did not grow in (c)-(e) and decreased in both length and interval in (e)-(f).

Simulated chain profiles with the Distinct Element Method are shown in Fig. 5. The results qualitatively agreed with the experimental observation that the length and interval increased in the field up to 0.1 T and then decreased in the field from 0.1 to 1.0 T.

The chain length and interval are plotted in Fig. 6 with respect to the magnetic flux density. As shown in Fig. 4 and 5, the length and interval increased with increase in magnetic field up to 0.1 T, then became almost constant from 0.1 to 0.6 T, and decreased in the extremely high field. These features can be explained by the concept of the potential energy minimization² because the numerical calculations, in which mechanical, magnetic and gravitational forces are included, agreed with the experimental results qualitatively. In addition, elastic energy of chains must be considered for the quantitative evaluation.

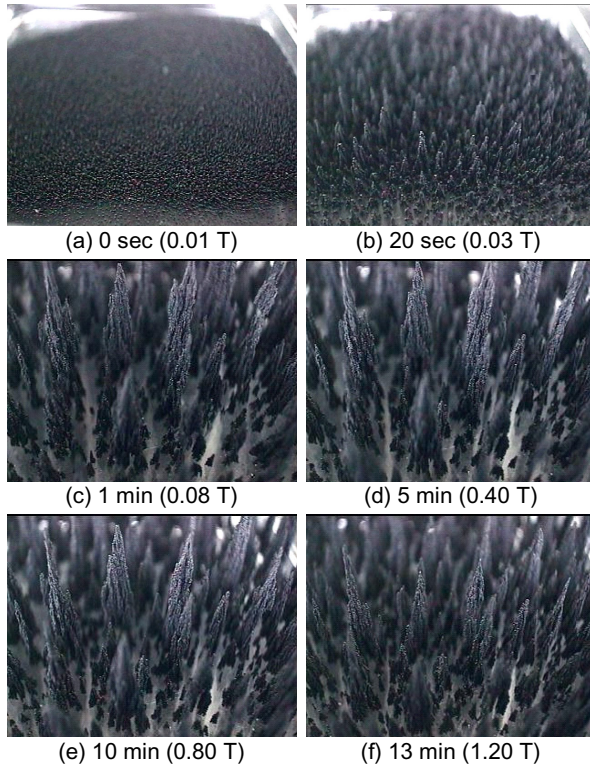


Figure 4. Profiles of chains in the experiment using superconducting coil.

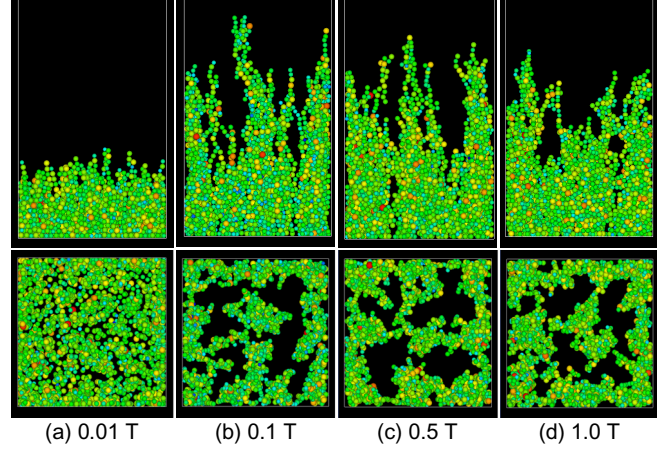


Figure 5. Simulated results of chain forming process.

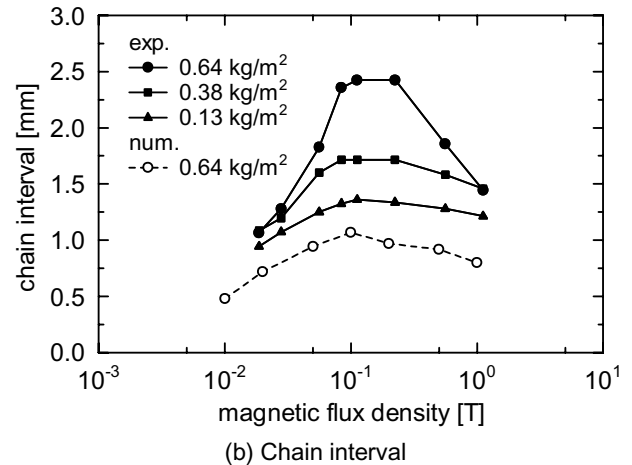
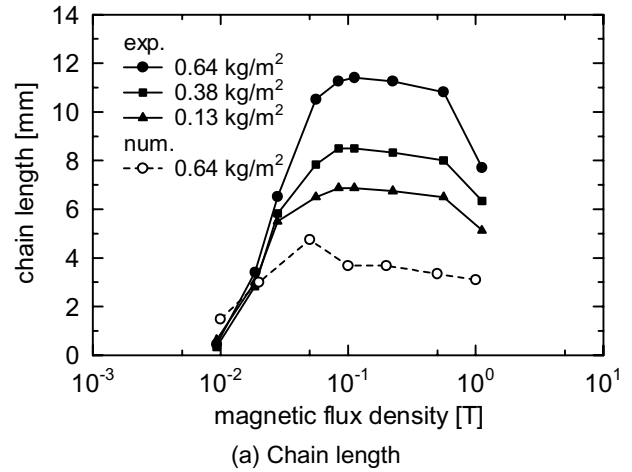


Figure 6. Chain length and interval varying with magnetic field.

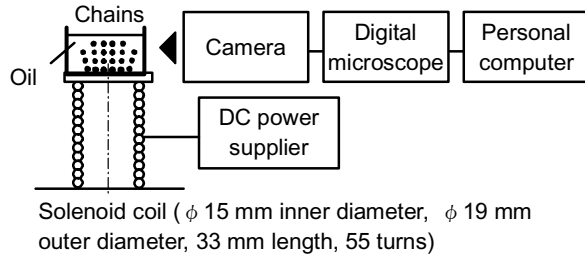


Figure 7. Experimental setup of chain formation in oil.

Chains in Oil

Experimental Method

Chain formation experiment in oil was carried out by a setup shown in Fig. 7. A solenoid coil was used as a generator of magnetic field. An axial component of the field at the top of the coil can be approximated by Eq. 6 but $B_0 = 6.16 \text{ mT/A}$ (B_0 is proportional to coil current) and $c = 66.87 \text{ 1/m}$. Formation of chains in commercial salad oil was observed by a digital microscope (Keyence Corp., VH-7000).

Results

The observed chain forming process in oil is shown in Fig. 8 comparing with that in air.³ Chains were formed in oil same as in air. However it took approximately two seconds to form chains while it took just 30 milliseconds in air. In addition, dispersion of beads by magnetic repulsive forces when the magnetic field was just applied was not observed in oil. These features in oil resulted from highly viscous force. As a result, thick and uniform chains were formed.

Simulated chain profiles in oil and in air are shown in Fig. 9. In the calculation for those in oil, the friction coefficient was set to zero and the viscous coefficient of oil was set to $0.1 \text{ Pa}\cdot\text{s}$. The experimental and numerical values of the chain formation time, length and interval are listed in Table 1. The formation times and intervals between chains are larger and chain lengths are smaller in oil than those in air. The simulated results agreed with the experimental results qualitatively. It was shown that these differences in the formation time and chain configurations were due to the difference in friction and viscosity in oil and in air.

Table 1. Comparison of Properties of Chains Formed in Oil with That in Air.

	Oil		Air	
	Exp.	Cal.	Exp.	Cal.
Viscous coefficient [$\mu\text{Pa}\cdot\text{s}$]	10^5	10^5	18.2	18.2
Formation time [s]	2.07	1.85	0.030	0.026
Chain length [mm]	2.36	0.97	3.61	1.68
Intervals of chain [mm]	0.56	0.38	0.41	0.35

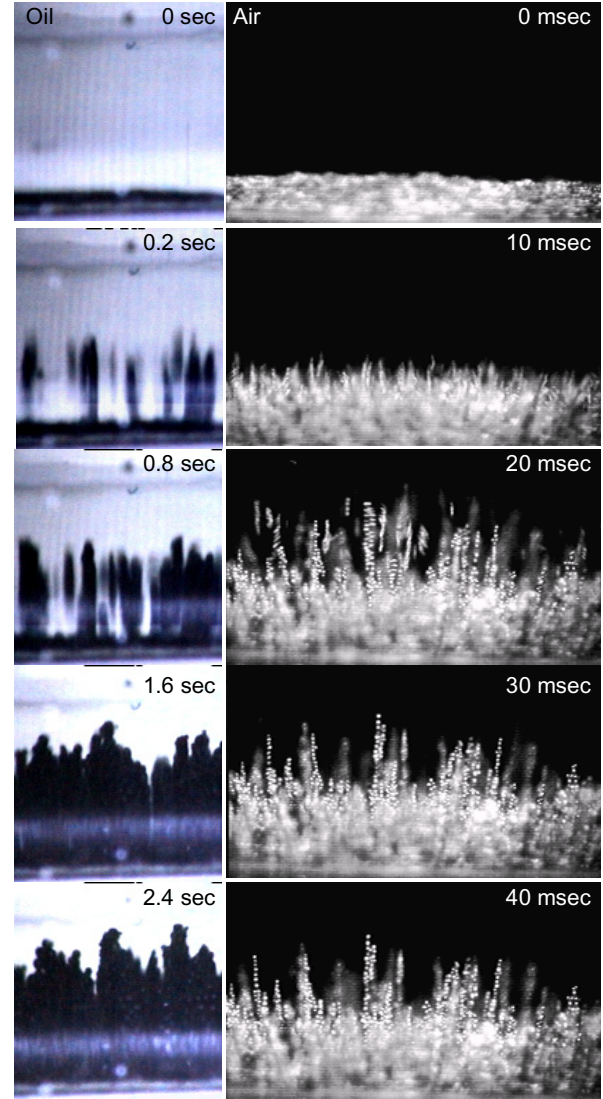


Figure 8. Comparison of chain forming process in oil with that in air.

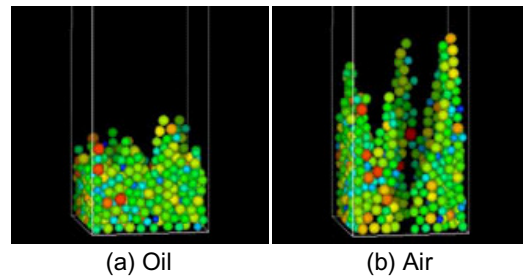


Figure 9. Comparison of simulated profiles of chains in oil with that in air.

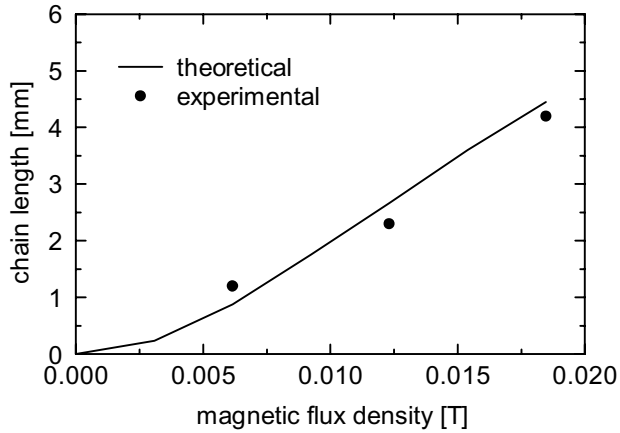


Figure 10. Comparison of theoretically estimated chain length with experimental results.

The theoretically estimated chain length and experimental results in oil are plotted in Fig. 10. The theoretical values were calculated by the potential energy minimization theory, where a single line shaped chain shown in Fig. 2 (a) was assumed and the effect of friction was neglected.² In this experiment, sufficient beads more than 0.64 kg/m^2 were provided in order to prevent lack of beads to form thick chains. From the results, it was shown that theoretical values agreed with the experimental quantitatively, because the effect of friction was negligible.

Chains with Toner Particles

Experimental Method

Experimental setup for the chain length measurement using carrier beads with toner particles was similar to that described in Fig. 7 except that oil did not used for this experiment, $B_0 = 14.15 \text{ mT/A}$ and $c = 61.43 \text{ 1/m}$. The electric pull-off characteristics of chains with toner particles were measured with the setup shown in Fig. 11. The electric field was applied statically to chains between a set of parallel electrodes with 6.0 mm in gap. When the sufficient electric field was applied, carrier beads at the top of chains were charged and pulled off by the electrostatic force. The critical voltage between electrodes to break chain was recorded and it was converted to the electric field intensity.

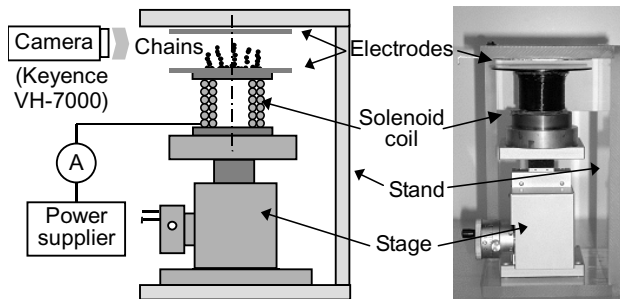


Figure 11. Experimental setup for electric pull-off of chains.

Results

Figure 12 shows the measured chain length with and without toner particles for $88 \mu\text{m}$ carrier beads. Toner concentration was set at 10 wt%. The lengths did not vary by the introduction of toner particles. The results were compared to the values calculated by the potential energy minimization theory of the single chains as shown in Fig. 2 (a) and (b). In the case with toner particles, each separation between carrier beads was equal to the diameter of a toner particle, $5 \mu\text{m}$. It was confirmed that toner particles did not affect the chain length.

Electric field intensity to break chains is plotted in Fig. 13 as a function of toner concentration. The critical electric field increased significantly by the introduction of insulative toner particles into conductive carrier beads. In addition, discontinuous variation is observed in the figure around 6-8 wt% concentration. The result depended on how many toner particles were attached to a carrier bead and it is supposed to correspond to the resistance of chains. In Fig. 14, measured resistance of a composite layer with carrier beads and toner particles are plotted. The layer was 1 mm in thickness and 10 mm in diameter. The curve is similar to that shown in Fig. 13.

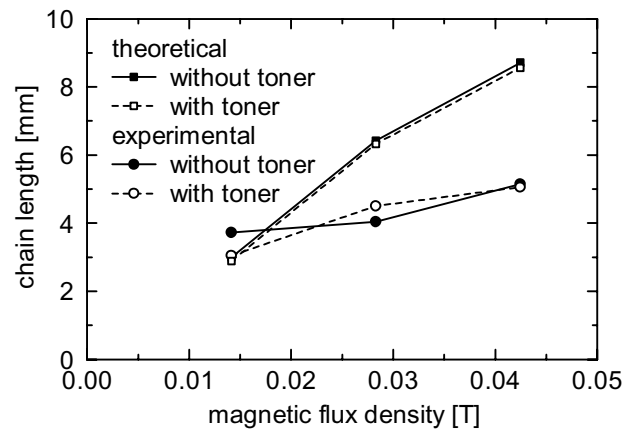


Figure 12. Measured and theoretically estimated chain length with and without toner particles.

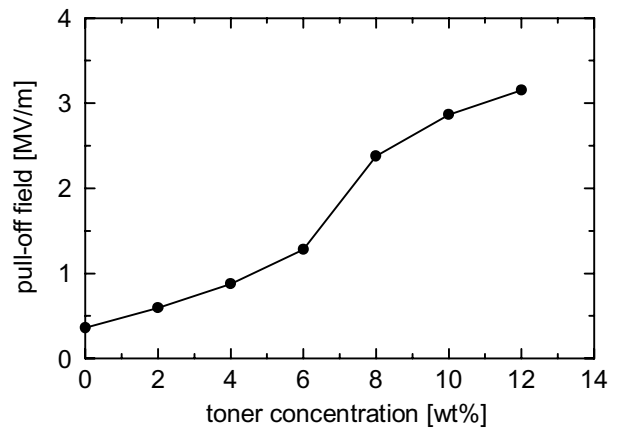


Figure 13. Electric field intensity to break chains as a function of toner concentration.

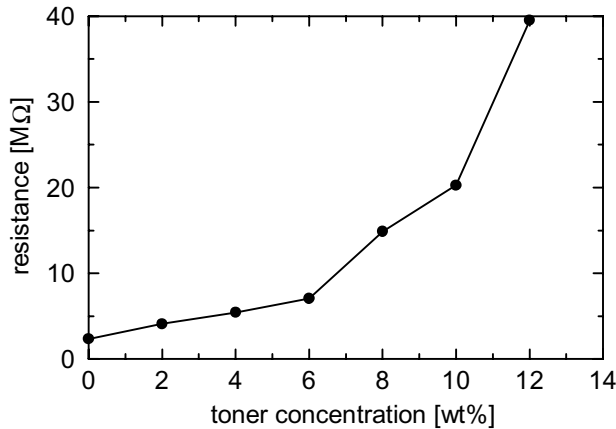


Figure 14. Resistance of composite layer of carrier beads and toner particles as a function of toner concentration.

Conclusion

The effects of magnetic field, friction, and introduction of toner particles on the properties of carrier bead chains were investigated by three kinds of independent studies. It was clarified that (1) lengths and intervals of chains increased with the increase in magnetic field until 0.1 T but it decreased in the higher field, (2) properties of chains formed in oil are different from those formed in air by the difference in friction and drag forces, and the measured length agree with the theoretical values quantitatively and (3) introduction of toner particles makes chains highly resistive and pull-off field increase significantly while they do not affect the lengths of chains.

References

1. E. M. Williams, *The Physics and Technology of Xerographic Processes*, Krieger Publishing, FL, 1993.
2. N. Nakayama, H. Kawamoto and M. Yamaguchi, Statics of Magnetic Bead Chain in Magnetic Field, *J. Imaging Sci. Technol.*, 46, 5 (2002), 422-428.
3. N. Nakayama, H. Kawamoto and M. Yamaguchi, Resonance Frequency and Stiffness of Magnetic Bead Chain in Magnetic Field, *J. Imaging Sci. Technol.*, 47, 5 (2003), 408-417.
4. Nobuyuki Nakayama, Yoichi Watanabe, Yasuaki Watanabe and Hiroyuki Kawamoto, Experimental and Numerical Study on the Bead-Carry-Out in Two-Component Development Process in Electrophotography, *IS&T's NIP19: The 19th International Conference on Digital Printing Technologies*, (2003), 69-73.
5. R. S. Paranjpe and H. G. Elrod, Stability of Chains of Permeable Spherical Beads in an Applied Magnetic Field, *J. Appl. Phys.*, 60, 1 (1986), 418-422.
6. P. A. Cundall and O. D. L. Strack, A Discrete Numerical Model for Granular Assemblies, *Géotechnique*, 29, 1 (1979), 47-65.

Biography

Nakayama, Nobuyuki holds a BS degree in Physics from Tohoku Univ. (1983) and a Dr. degree in Mechanical Engineering from Waseda Univ. (2003). In 1983, he joined Fuji Xerox Co., Ltd., where he has been engaged in a research on electrophotography and is currently studying on powder dynamics. He is an associate researcher of Waseda Univ., and a member of the Imaging Society of Japan and the Japan Society of Mechanical Engineers.